

Appendix A Application of Thermocouples in Steady Laminar Flames

Despite the simplicity of thermocouple theory [Wright, 1995] and construction, thermocouple thermometry in combustion environments is anything but simple. Transient and steady heat and mass transfer phenomena can cause the measured surface temperature of the thermocouple to be considerably different from the desired local gas temperature.

A.1 Thermocouple Thermal Capacitance

When a thermocouple junction is suddenly immersed into a fluid stream at a different temperature the measured junction temperature will vary with time asymptotically approaching an equilibrium value where $dT/dt = 0$. The transient behavior of a thermocouple junction may be approximated using the lumped capacitance first order model

$$-hA_s(T(t) - T_\infty) = \rho V c \frac{dT}{dt} \quad \text{Equation A.1}$$

with the solution

$$\frac{T(t) - T_\infty}{T_{\text{initial}} - T_\infty} = \exp\left[-\left(\frac{hA_s}{\rho V c}\right)t\right] \quad \text{Equation A.2}$$

where

h	=	junction heat transfer coefficient
A_s	=	junction surface area
V	=	effective junction volume
c	=	junction material specific heat

r	=	junction material density
t	=	time
$T(t)$	=	junction temperature at time t
T_{initial}	=	junction temperature at time $t = 0$
T_{∞}	=	free stream gas temperature

This model works well when only one heat transfer mode (conduction, convection or radiation) is acting on the thermocouple and when temperature gradients inside the thermocouple are small. Temperature gradients may be considered negligible for Biot numbers less than 0.1 which is typically the case for thermocouple junctions.

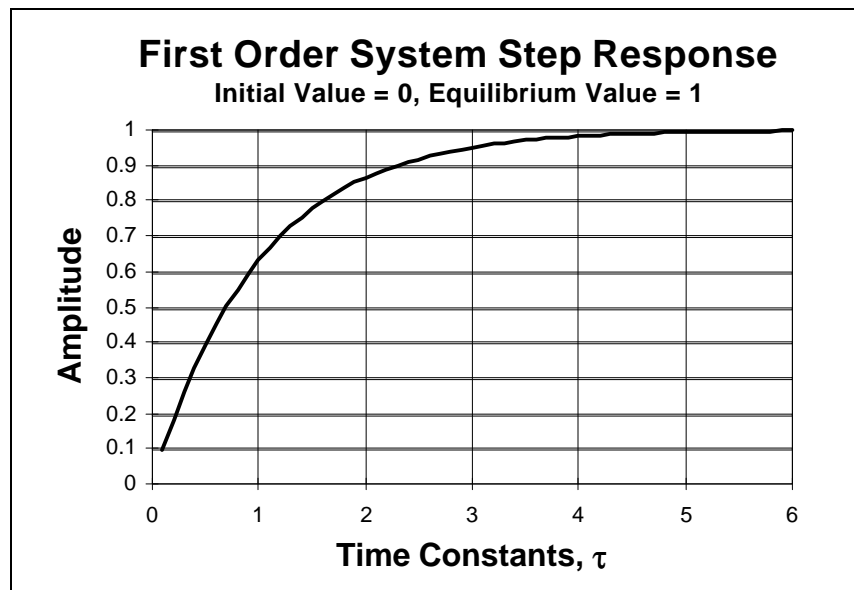


Figure A.1 First Order System Step Response

From the results of the first order model a time constant, τ , may be defined which characterizes the transient behavior of the thermocouple

$$\tau = \frac{\rho V c}{h A_s} \quad \text{Equation A.3}$$

The thermocouple time constant may also be defined experimentally. Differentiating Equation A.2 once with respect to time and using linear regression to estimate the slope of

$$-\tau = \frac{d}{dt} \left[\ln \left(\frac{T(t) - T_{\infty}}{T_{\text{initial}} - T_{\infty}} \right) \right] \quad \text{Equation A.4}$$

where the logarithm term of Equation A.4 versus time will be linear for true first order behavior.

Multiple mode heat transfer involving the thermocouple junction, typically found in combustion environments, tends to invalidate the first order model because there are several driving temperature differences, i.e. $T_{\infty, \text{conduction}}$, $T_{\infty, \text{convection}}$ and $T_{\infty, \text{radiation}}$. To effectively model the transient behavior for a thermocouple undergoing multiple modes of heat transfer it is best to use an implicit model.

A.2 Thermocouple Thermometry in Non-Sooting Flames

It is important to note that thermal equilibrium does not necessarily imply that all heat transfer involving the junction has ceased but rather the *rates* of conductive, convective and radiative heat transfer have become *steady with time*. Most commonly when a thermocouple is in thermal equilibrium with a non-sooting combustion environment heat steadily flows by convection from the surrounding gas into the junction balanced by lead wire conduction and radiation with cooler surroundings steadily drawing heat away from the junction as stated in Equation A.5. These heat transfer processes can cause differences between the thermocouple temperature and the gas temperature of several hundred Kelvin.

$$\dot{q}_{\text{convection}} = \dot{q}_{\text{radiation}} + \dot{q}_{\text{conduction}} \quad \text{Equation A.5}$$

The effects of lead wire conduction can be minimized through the choice of thermocouple geometry and experiment design. By increasing the length of thermocouple wire in crossflow to be much larger than the wire diameter conduction effects can be minimized. Collis and Williams [1959] recommends wire (length / diameter) ≥ 1000 to thermally isolate the middle of the wire from end effects. Conduction effects may also be minimized by choosing, whenever possible, to align the length of wire in crossflow along an isotherm as is commonly done in two dimensional flames such as Tsuji counterflow burners and Wolfhard-Parker coflowing slot burners. Analytical heat transfer calculations by Bradley and Matthews [1968] showed that errors due to conduction effects could be reduced to less than 0.1 % for 12.5 μm uncoated thermocouple wire 5 mm long (length / diameter = 400) aligned along an isotherm in a flame. Based on their calculations for coated wires with a final diameter of 100 μm Bradley and Matthews [1968] recommended doubling the thermocouple length to 10 mm (length / diameter = 100). The remaining discussion will neglect thermocouple lead wire conduction effects.

Using conservation of energy for a thermocouple in equilibrium with its surroundings as stated in Equation A.6 and quantitative information about the convection

$$\dot{q}_{\text{convection}} = \dot{q}_{\text{radiation}} \quad \text{Equation A.6}$$

and radiation heat transfer process one can calculate the difference between the measured thermocouple temperature and the local gas temperature. With knowledge of the thermocouple's radiant emissivity, ϵ , thermocouple surface temperature and the

temperature of the surroundings one can estimate the radiant heat flux away from the junction by using Equation A.7

$$q''_{\text{radiation}} = \sigma \epsilon (T_{\text{tc}}^4 - T_{\text{surr}}^4) \quad \text{Equation A.7}$$

where σ = Boltzman constant; $5.67 \times 10^{-8} \text{ W/m}^2 \cdot \text{K}$

Checking the relative magnitudes of the fourth power of the surroundings temperature versus the fourth power of the thermocouple temperature one might choose to neglect the surrounding's temperature term. It is tempting to consider the flame under investigation as a radiating surface in the temperature correction but analysis usually shows that laboratory scale flames do not make a significant contribution. Although the combustion gases and soot particles are at very high temperatures, short mean beam lengths in laboratory scale flames usually limits their emissivity to < 0.1 .

Using empirical correlations to quantify the heat transfer coefficient, h , in the convective term of Equation A.6

$$q''_{\text{convection}} = \bar{h} (T_{\text{gas}} - T_{\text{tc}}) \quad \text{Equation A.8}$$

where
$$\bar{h} = \frac{\bar{Nu}_d \cdot k_{\text{gas}}}{d} \quad \text{Equation A.9}$$

$$\bar{Nu}_d = f(\text{Re}_d, \text{Pr}), \text{ empirical correlation} \quad \text{Equation A.10}$$

and
$$\begin{aligned} \text{Nu}_d &= \text{Nusselt Number} \\ \text{Re}_d &= \text{Reynolds number} \\ \text{Pr} &= \text{Prandtl number} \\ k_{\text{gas}} &= \text{gas thermal conductivity} \\ d &= \text{thermocouple junction diameter} \end{aligned}$$

Empirical Nusselt number relations exist for flows over various geometries (i.e. spheres, infinite cylinders...) and the correct expression depends on accurate characterization of the thermocouple junction geometry. A detailed discussion of typical thermocouple convection properties is presented later in section A.5. This analysis will proceed under the assumption that the thermocouple Nusselt number is known. From Equations A.6 - A.10 the gas temperature may be calculated as

$$T_{\text{gas}} = T_{\text{tc}} + \sigma \epsilon \left(T_{\text{tc}}^4 - T_{\text{surr}}^4 \right) \frac{d}{\text{Nu}_d \cdot k} \quad \text{Equation A.11}$$

A.3 Thermocouple Thermometry in Sooting Flames

The preceding analysis for radiation correction to thermocouple measurements in combustion environments is only valid for non-sooting flames. Thermocouple thermometry in sooting flames is complicated even further by mass transport of soot from the gas flow to the thermocouple surface [Eisner and Rosner, 1985]. When a clean thermocouple is placed into a sooting flame thermophoresis dominates the soot transport to the thermocouple surface [McEnally *et. al.*, 1997] and is augmented by coagulation and surface growth reactions identical to those that soot particles in the flow naturally experience.

Thermophoresis is a diffusion process that tends to drive particles in a temperature gradient from hot to cold. This process may be easily rationalized by the kinetics of gases in a temperature gradient. One can imagine that a particle in a temperature gradient will have more molecular collisions on its hot side than cold side with the resulting

conservation of momentum driving the particle from hot to cold. Since a thermocouple in thermal equilibrium with a combustion gas stream typically experiences steady convective heating by the surrounding gas there also must exist a temperature gradient dropping from the free stream temperature to a lower thermocouple surface temperature. This convective temperature gradient surrounding the thermocouple is the thermophoretic driving potential.

With continuous mass transport of soot from the gas stream to the thermocouple surface affecting the heat transfer process via changes in thermocouple Nusselt number and radiant emissivity the thermocouple junction never achieves thermal equilibrium with its surroundings. Transient analysis of thermocouple measurements in sooting flames is required to determine the gas temperature.

Figure A.2 taken from McEnally *et. al.* [1997] shows a typical time trace for a clean thermocouple inserted into a sooting flame. The transient behavior of the thermocouple is first dominated by its thermal capacitance followed by soot transport effects. The initial effect of soot deposition on the thermocouple is to gradually change its radiant emissivity with negligible change to the thermocouple's diameter. Using platinum alloy thermocouples their emissivity will vary from approximately 0.2 clean to nearly 1.0 (blackbody) coated with soot. Variations in the thermocouple's diameter, and therefore Reynolds number and Nusselt number, from soot deposition dominate the response after the variable emissivity region. The end of the variable emissivity region and beginning of the variable diameter region is usually identified by an abrupt change in the slope of the temperature profile seen in Figure A.2 at about 5 seconds.

Rapid insertion temperature measurement algorithms are reported in the literature [Kent and Wagner, 1984, Govatzidakis, 1993 and McEnally *et. al.*, 1997] as methods to determine what a thermocouple's equilibrium temperature *would have been* in the absence of soot in the hot gas stream. Rapid insertion temperature measurement in sooting flames (as the name implies) involves rapidly translating a clean thermocouple from outside the flame to a location in the flame where the gas temperature is desired. The thermocouple is left stationary in the flame while a time trace of its temperature history is recorded (several seconds). When data collection is complete the thermocouple is retracted to an aggressively oxidizing region of the flame where the soot is burned off of the thermocouple in preparation for the next measurement.

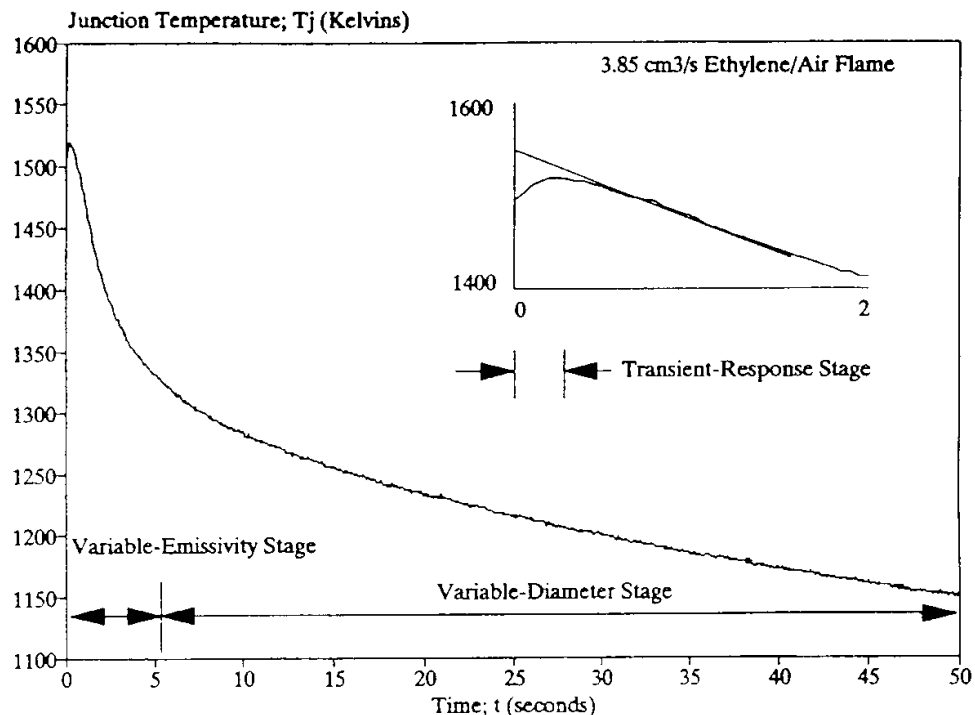


Figure A.2 Thermocouple Time Trace in a Sooting Flame [McEnally *et. al.*, 1997]

With the radiant emissivity and convective heat transfer coefficient of the thermocouple changing in time the only time that these quantities are well known is at the time of insertion, $t = 0$. Linear extrapolation of the variable emissivity region of the temperature profile to time zero (instant of insertion) can be used as an estimate of what the thermocouple equilibrium temperature would have been in the absence of soot deposition [Govatzidakis, 1993]. The local gas temperature can now be calculated based on the “time zero” thermocouple temperature approximation and the clean radiative and convective heat transfer properties using Equations A.6 - A.11 as discussed previously.

A.4 Thermocouple Particle Densitometry

A technique recently developed by McEnally *et. al.* [1997] called Thermocouple Particle Densitometry (TPD) can be used to extract the actual value of the local soot volume fraction from thermocouple time traces in sooting flames. TPD involves fitting measured temperature time traces in the variable diameter region to an analytical thermophoretic transport model yielding local soot volume fraction. Analysis shows that thermophoresis is the dominant mass transport mechanism for soot deposition on the thermocouple [McEnally *et. al.*, 1997]. Advantages of this method over optical absorption techniques is that the measurement is independent of the soot size, morphology and optical properties and does not require line of sight optical access to implement.

The following is an abbreviated summary of TPD analysis developed in detail in McEnally *et. al.* [1997]; the interested reader is encouraged to review the article. By conservation of energy for a thermocouple junction in quasi-steady equilibrium

$$\epsilon_j \sigma T_{tc,j}^4 = \frac{k_{g0} \cdot \bar{Nu}_j}{2d_{tc}} (T_{gas}^2 - T_{tc,j}^2) \quad \text{Equation A.12}$$

where j = index indicating j^{th} sample in temperature/time trace
 k_{g0} = k_g / T_{gas} = constant value $6.54 \times 10^{-5} \text{ W/mK}^2$

Equations A.11 and A.12 express the same idea with the only differences being that Equation A.12 neglects the surroundings temperature in the radiation term and that the convection term is stated in terms of *heat flux potentials* [Rosner, 1986] taking advantage of the linearity of k_g with temperature. Equation A.12 applied to the extrapolated zeroth data point of the temperature profile as discussed in section A.3 yields an estimate of the local gas temperature.

The thermophoretic soot mass flux from the free stream to the thermocouple surface, j'' , can be expressed as

$$j'' = (D_T \bar{Nu}_j f_v \rho_P / 2d_{tc,j}) \left(1 - (T_{tc,j} / T_{gas})^2 \right) \quad \text{Equation A.13}$$

where $D_T = \frac{3}{4} (1 + \pi \alpha_{mom} / 8)^{-1} \nu_{gas}$ Equation A.14

and

- D_T = thermophoretic diffusivity
- f_v = soot volume fraction
- ρ_P = intrinsic density of soot particles
- α_{mom} = momentum accommodation coefficient ≈ 1
- ν_{gas} = gas kinematic viscosity
- = $1.29 \times 10^{-9} T_{gas}^{1.65} \text{ m}^2/\text{s}$

By conservation of mass the soot mass flux, j'' , can be related to the change in diameter of either a cylinder or sphere as

$$j'' = \frac{\rho_d}{2} \frac{d(d_{tc,j})}{dt} \quad \text{Equation A.15}$$

where ρ_d = soot deposit density

It is important to note that the intrinsic density of soot particle in the free stream, ρ_p , is different from the soot deposit density, ρ_d . Measurements by [Choi *et. al.*, 1995] estimate $\rho_d / \rho_p = \varphi = 0.095 \pm 0.04$.

Assuming ε_j and Nu_j to be constant with time during the variable diameter stage Equation A.12 may be differentiated with respect to time to yield

$$\frac{d(d_{tc,j})}{dt} = \left(\frac{k_{g0} \bar{Nu}}{\varepsilon_{soot} \sigma} \right) \left(T_{tc,j}^{-3} - 2T_{gas}^2 T_{tc,j}^{-5} \right) \frac{dT_{tc,j}}{dt} \quad \text{Equation A.16}$$

Assuming ε_j constant at the value of *soot* emissivity (~ 0.95) in the variable diameter region is a very good assumption. Assuming the thermocouple Nusselt number to remain constant in the variable diameter region is marginal at best but attractive considering the simplicity it offers. Equations A.12, A.13, A.15 and A.16 are combined to form a differential equation which may be integrated to yield

$$G = mt + G(t = 0) \quad \text{Equation A.17}$$

$$\text{where } G \equiv \frac{1}{4} \left(\frac{T_{gas}}{T_{tc,j}} \right)^8 - \frac{1}{6} \left(\frac{T_{gas}}{T_{tc,j}} \right)^6 \quad \text{Equation A.18}$$

$$m \equiv \beta \cdot f_v \quad \text{Equation A.19}$$

$$\beta \equiv 2D_T \varepsilon_{soot} \sigma^2 T_{gas}^4 / (\phi k_{g0}^2 \bar{Nu}) \quad \text{Equation A.20}$$

The transformation of Figure A.2 into $G(t)$ coordinates is shown below in Figure A.3.

Solution Outline:

1. Transform measured $(T_{ic,j}, t)$ data pairs into (G_j, t) pairs using Equation A.17 along with the calculated gas temperature, T_{gas}
2. approximate m by linear regression of $G(t)$ over the variable diameter region
3. calculate the soot volume fraction, f_v , from Equation A.19

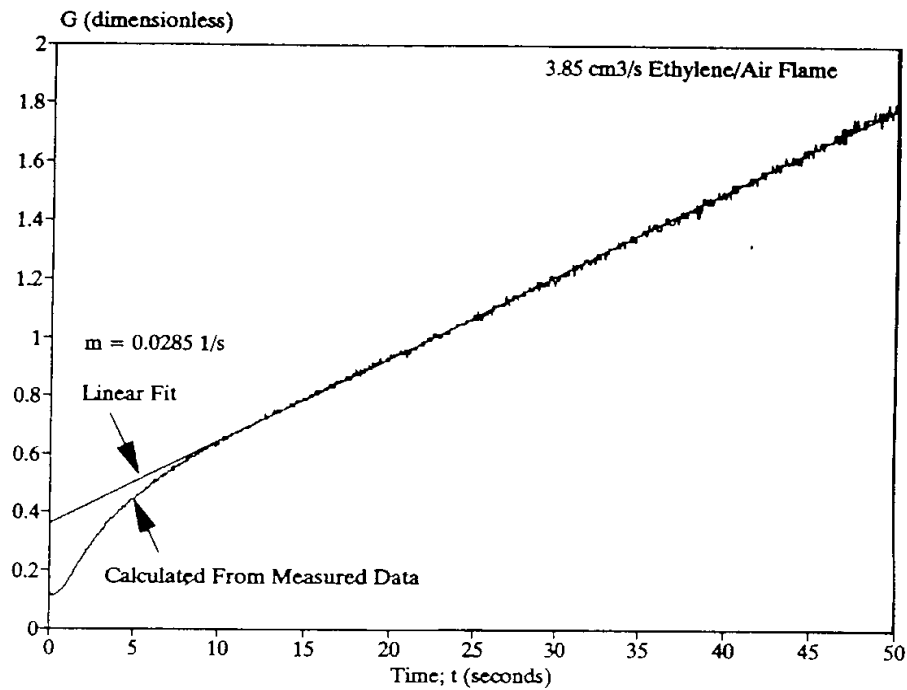


Figure A.3 $G(t)$ Transformation of $T(t)$ [McEnally *et. al.*,1997]

A.5 Convection Heat Transfer Properties of Thermocouple Junctions

Application of any of the ideas in the previous sections of this appendix require detailed knowledge of the thermocouple junction's convective heat transfer characteristics. Accurate models for the thermocouple's convective heat transfer coefficient, h , or Nusselt number, Nu_d , (h and Nu_d related by Equation A.9) are needed. Historically the convective behavior of thermocouple junctions were derived from empirical relations for infinite cylinders [Whitaker, 1972] or spheres [Collis and Williams, 1959]. The decision of whether a thermocouple junction behaved similar to that of a cylinder or sphere was typically made based on a visual *qualitative* judgment of its junction diameter, d_j , relative to the lead wire diameter, d_w . Clearly for large d_j/d_w the junction would behave much like a sphere and for $d_j/d_w \rightarrow 1$ more like a cylinder.

Empirical convective heat transfer relations typically used to model thermocouple junctions are shown below in Equations A.21 and A.22.

from Collis and Williams [1959]

$$Nu_{d, \text{cylinder}} = \left[A + BR^n \right] \left(\frac{T_m}{T_\infty} \right)^{0.17} \quad \text{Equation A.21}$$

where $T_\infty \equiv$ free stream temperature
 $T_m \equiv$ "film temperature" = $(T_\infty + T_0) / 2$

Table A.1 Values of n, A and B for Equation A.21

	$0.02 < Re_d < 44$	$44 < Re_d < 140$
n	0.45	0.51
A	0.24	0
B	0.56	0.48

from Whitaker [1972]

$$\text{Nu}_{d,\text{sphere}} = 2 + \left(0.4 \text{Re}_d^{1/2} + 0.06 \text{Re}_d^{2/3}\right) \text{Pr}^{0.4} \left(\mu_\infty / \mu_0\right) \quad \text{Equation A.22}$$

where $\mu_0 \equiv$ fluid dynamic viscosity at the junction surface temperature
 $\mu_\infty \equiv$ fluid dynamic viscosity at the free stream temperature

for $0.71 < \text{Pr} < 380$
 $3.5 < \text{Re}_d < 7.6 \times 10^4$
 $1.0 < (\mu_\infty / \mu_0) < 3.2$

All fluid properties in Equation A.21 are evaluated at the film temperature, T_m , and the properties used in Equation A.22 are evaluated at the free stream temperature, T_∞ , unless otherwise subscripted. Examining the plots of Equations A.21 and A.22 versus Reynolds number in Figure A.4, notice that as $\text{Re}_d \rightarrow 0$ (free convection), $\text{Nu}_{d,\text{cyl}} \rightarrow 0$ but $\text{Nu}_{d,\text{sph}} \rightarrow 2.0$. The limiting value of Nusselt number for spheres at small Reynolds numbers is not intuitively obvious but is analytically based [Acrivos and Taylor, 1962] and experimentally verified [Vliet and Leppert, 1961]. Notice also how the ratio of $\text{Nu}_{\text{cyl}} / \text{Nu}_{\text{sph}}$ rapidly decreases for small Reynolds numbers further illustrating fundamental differences in the convection behavior of these two geometries.

From Figure A.5 one can see that for small Reynolds numbers, $\text{Re}_d < 10$, typical of laboratory scale laminar flames, the choice of cylindrical versus spherical thermocouple junction convective heat transfer models can make a difference of *hundreds of degrees* in the calculated gas temperatures. The most extreme consequences of these differences are realized in counterflow flames where the flame front lies near a true stagnation plane, Re_d

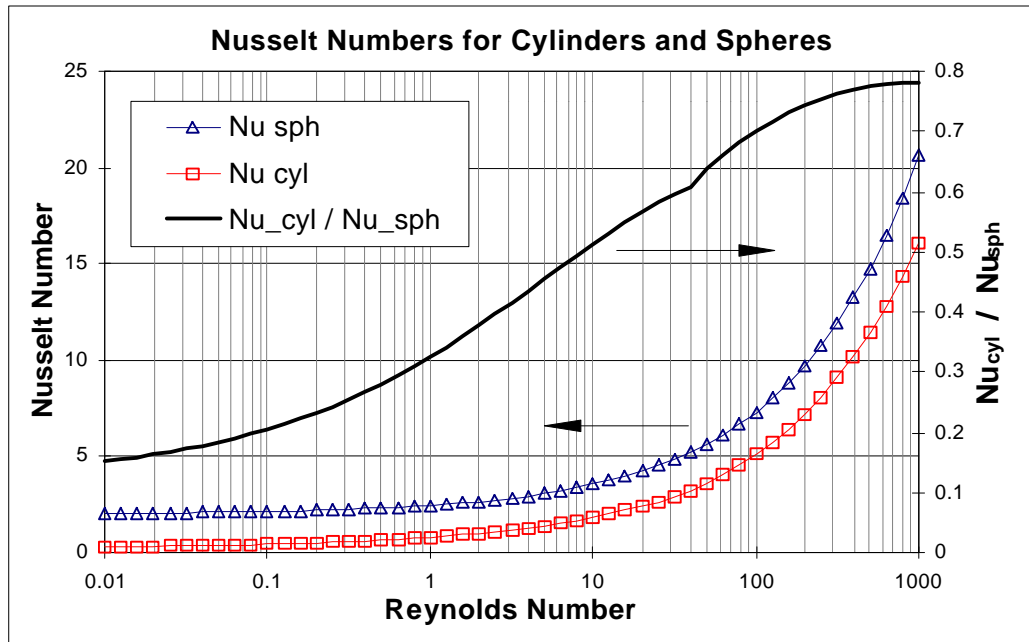


Figure A.4 Nusselt Numbers for Infinite Cylinders and Spheres vs. Reynolds Number

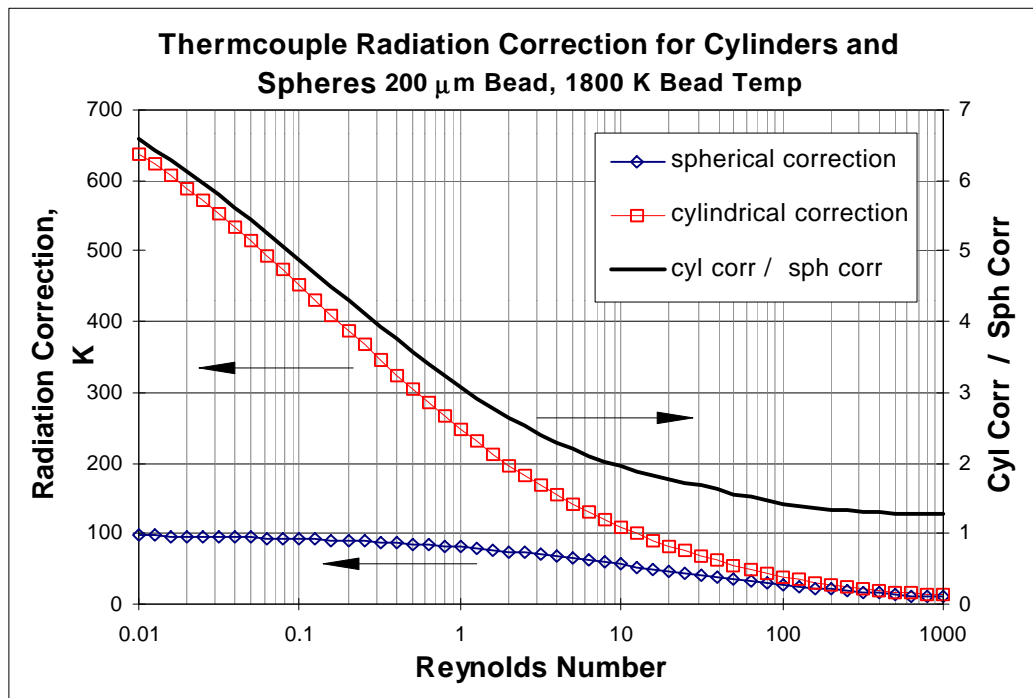


Figure A.5 Thermocouple Radiation Corrections for Cylindrical and Spherical Junction Convection Models

= 0 (free convection). Figure A.6 shows that soot volume fractions measured via TPD appear to vary linearly with junction Nusselt number.

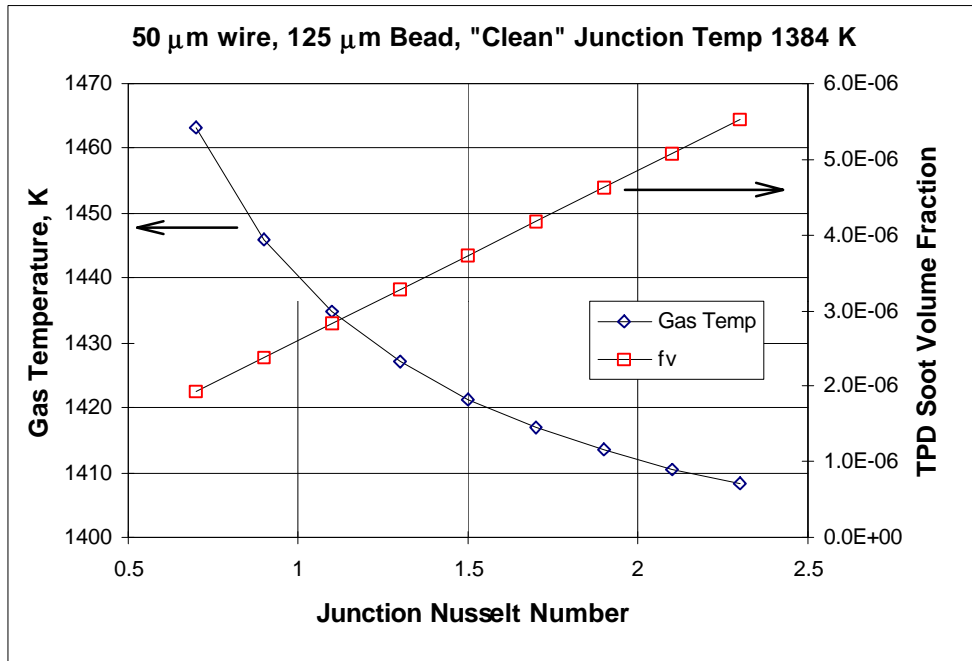


Figure A.6 TPD Soot Volume Fraction Sensitivity to Junction Nusselt Number

The drastic differences between these two convection models merits a closer look at typical thermocouple construction in relation to the idealized models for infinite cylinders and spheres. One could certainly construct a thermocouple with a junction diameter much larger than the lead wire stock having essentially spherical convective heat transfer behavior as shown in figure A.7C. However, spherical junctions have large thermal capacitance and poor spatial resolution making them undesirable for combustion research. Ideally thermocouples would have a purely cylindrical construction identical to that in Figure A.7A. In practice a perfectly cylindrical junction is nearly unattainable.

Even butt welding the wires together (a very difficult procedure) yields a junction with $d_j / d_w \approx 1.5$ at best with the compounding complication of “necking” at the root of the junction as one tries to make the junctions smaller. This dilemma in thermocouple fabrication once again leads to the question of whether practical thermocouple junctions, even those with the smallest diameters relative to the lead wire diameter, behave as cylinders or spheres. From figure A.7 one could argue that a typical thermocouple junction’s convective heat transfer characteristics could lie *somewhere between* those of infinite cylinders and spheres, which is the topic for the remainder of this section.

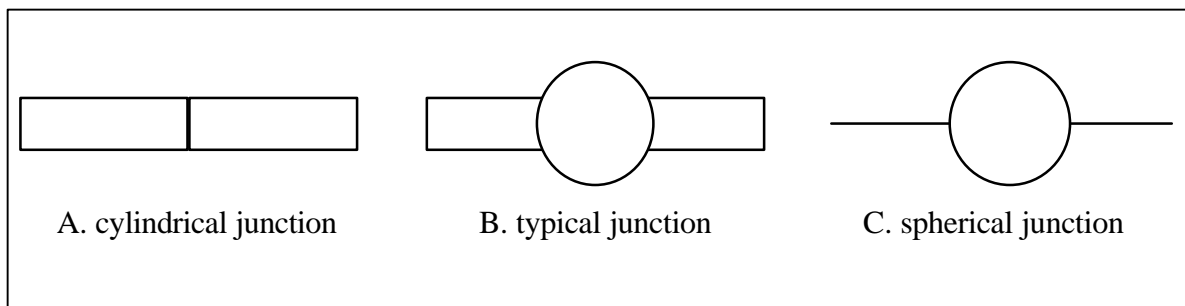


Figure A.7 Schematic representation of a typical thermocouple junction relative to cylindrical and spherical idealisms

Although large, virtually spherical junctions have undesirable characteristics with respect to combustion research one could possibly fabricate an arbitrarily large junction that could be treated as a standard with respect to its convective properties. With a standard established one could measure the convective properties of other junctions by measuring their surface temperatures in identical high temperature gas streams.

The thermocouple junction shown in Figure A.8 was an attempt to create a standard spherical thermocouple junction. It was constructed from 50 μm type B (Pt-

6%Rh / Pt-30%Rh) wire with $d_j / d_w = 8.8$ and was the largest the author could achieve without the junction having a “lumpy” appearance.

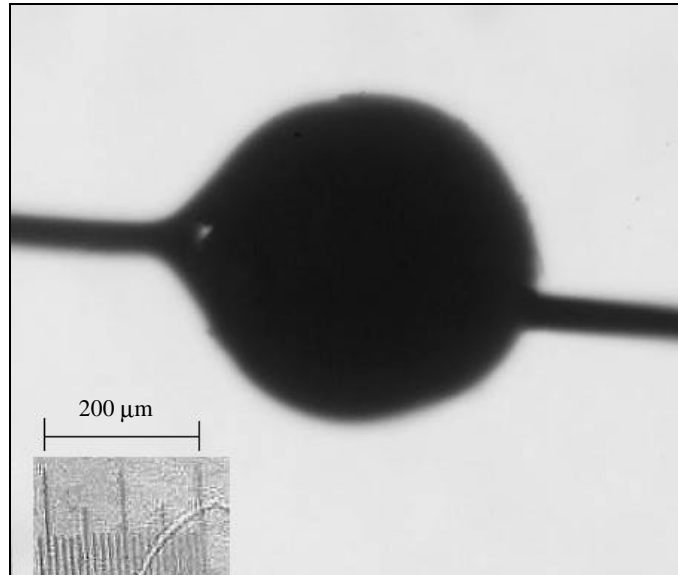


Figure A.8 Assumed Spherical Reference Thermocouple Junction, 50 μm wire, $d_j/d_w = 8.8$

Thermocouple Junction Nusselt Number Sample Calculation

Given:

- A spherical reference thermocouple, shown in Figure A.8, is placed in a Hydrogen/Air/Oxygen premixed flame with *reactant* velocity at STP of 8.126 cm/s
- measured surface temperature of the reference junction is $T_{s, \text{ref}} = 1295 \text{ K}$
- $(MW_{\text{reactants}}/MW_{\text{products}}) = 0.822$
- The thermocouple shown in Figure A.9 is placed in the same location of the same premixed flame and a thermocouple surface temperature of $T_{s, i} = 1287 \text{ K}$ is measured, where the subscript i indicates the i^{th} specimen which was compared to the reference

Find:

Nusselt number of the specimen thermocouple, $Nu_{\text{rel}, i}$, relative to the reference thermocouple's Nusselt number $Nu_{\text{sph}, \text{ref}}$

Assume:

1. perfectly spherical convective behavior for the reference junction
2. premixed flame products properties are identical to that of air at the same temperature and behave as an ideal gas
3. the hydrogen/air/oxygen premixed flame product's temperature is sufficiently small to neglect catalytic effects on the surface of the thermocouples' junctions [Kaskan, 1957]

Solution:

Conservation of Mass

$$v_{\text{products}} = v_{\text{reactants}} \left(\frac{MW_r}{MW_p} \right) \left(\frac{T_{\text{gas}}}{T_{\text{stp}}} \right) = \left(0.08126 \frac{\text{m}}{\text{s}} \right) (0.82168) \left(\frac{T_{\text{gas}}}{300\text{K}} \right)$$

Conservation of Energy from Equation A.11 for reference junction

$$T_{\text{gas}} = T_{s,\text{ref}} + \sigma \epsilon \left(T_{s,\text{ref}}^4 - T_{\text{surr}}^4 \right) \frac{d_{\text{ref}}}{\overline{\text{Nu}}_{\text{sph,ref}} \cdot k}$$

Empirical Nusselt number relation from Equation A.22

$$\text{Nu}_{\text{sph,ref}} = 2 + \left(0.4 \text{Re}_{d,\text{ref}}^{1/2} + 0.06 \text{Re}_{d,\text{ref}}^{2/3} \right) \text{Pr}^{0.4} \left(\mu_{\infty} / \mu_0 \right)$$

iterations on T_{gas} yields:

$$\begin{array}{llll} T_{\text{gas}} & = & 1361 \text{ K} & v_{\text{products}} = 30.3 \text{ cm/s} \\ \text{Re}_{d,\text{ref}} & = & 0.6868 & \epsilon = 0.1945 \\ \text{Nu}_{\text{sph,ref}} & = & 2.3411 & \end{array}$$

Now with a trustworthy estimate of gas temperature calculated based on the reference thermocouple junction recalculate fluid properties based on specimen thermocouple film temperature.

Answer:

Conservation of Energy from Equation A.11 for specimen junction yields

$$\text{Nu}_{\text{rel},i} = \frac{\sigma \varepsilon (T_{s,i}^4 - T_{\text{surr}}^4)}{(T_{\text{gas}} - T_{s,i})} \frac{d_i}{k} = \underline{\underline{1.175}}$$

Now calculating Nusselt numbers for the specimen thermocouple from the empirical relations for cylinders and spheres (Equations A.21 and A.22 respectively) for comparison yields

$$\text{Nu}_{\text{cyl},i} = 0.881 \quad \text{and} \quad \text{Nu}_{\text{sph},i} = 2.353$$

As hypothesized earlier the convective characteristics of the specimen (typical) thermocouple lies somewhere between that of an infinite cylinder and a sphere in that

$$(\text{Nu}_{\text{cyl},i} = 0.881) < (\text{Nu}_{\text{rel},i} = 1.176) < (\text{Nu}_{\text{sph},i} = 2.353)$$

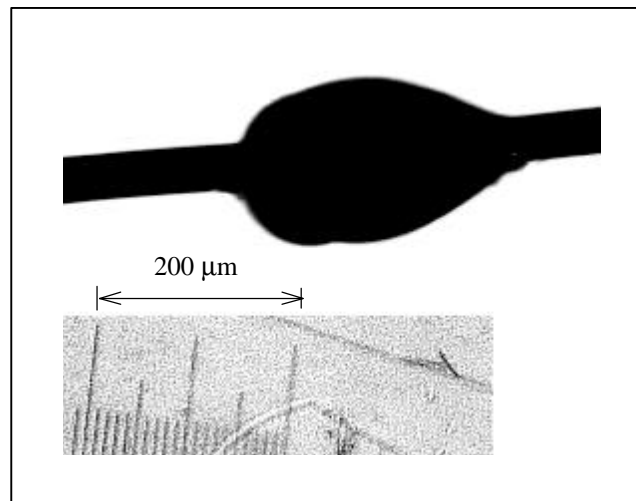


**Figure A.9 Thermocouple Junction Image for Sample Calculation,
50 μm wire, $d_j/d_w = 3.8$**

Normalizing the measured Nusselt number, $Nu_{rel,i}$, against those for cylinders and spheres by

$$\eta = \frac{Nu_{sph,i} - Nu_{rel,i}}{Nu_{sph,i} - Nu_{cyl,i}} = 0.8 \quad \text{Equation A.23}$$

where a value of $\eta = 1$ indicates cylindrical convective characteristics and a value of $\eta = 0$ indicates spherical convective characteristics.

Measuring the Nusselt numbers of thermocouples for an array of junction diameters, bare and SiO_2 coated, and plotting their normalized Nusselt numbers, η , versus a nondimensionalized diameter, d_j / d_w , yields the results in Figure A.10. Notice that for small values of $d_j / d_w \leq 2$ all of the junctions basically behave as infinite cylinders with a decreasing trend toward spherical behavior for increasing junction diameter as one would expect. This trend combined with the fact that nearly all of the measured Nusselt numbers fall between the cylindrical and spherical values (some slightly less than cylindrical values) tend to build confidence in the method.

Certainly, Figure A.10 would benefit from more data points. Continuation of this work should include parametric studies of the effect of varying the diameter of the reference junction and using an array of wire sizes. The end goal is to develop empirical relations based on trends like that shown in Figure A.10 to quantitatively characterize thermocouple junction convective properties. Information about the thermocouple's junction and wire sizes could be used in conjunction with empirical relationships for convection over infinite cylinders *and* spheres to reduce uncertainty in gas temperature calculations for combustion studies in laminar flames.

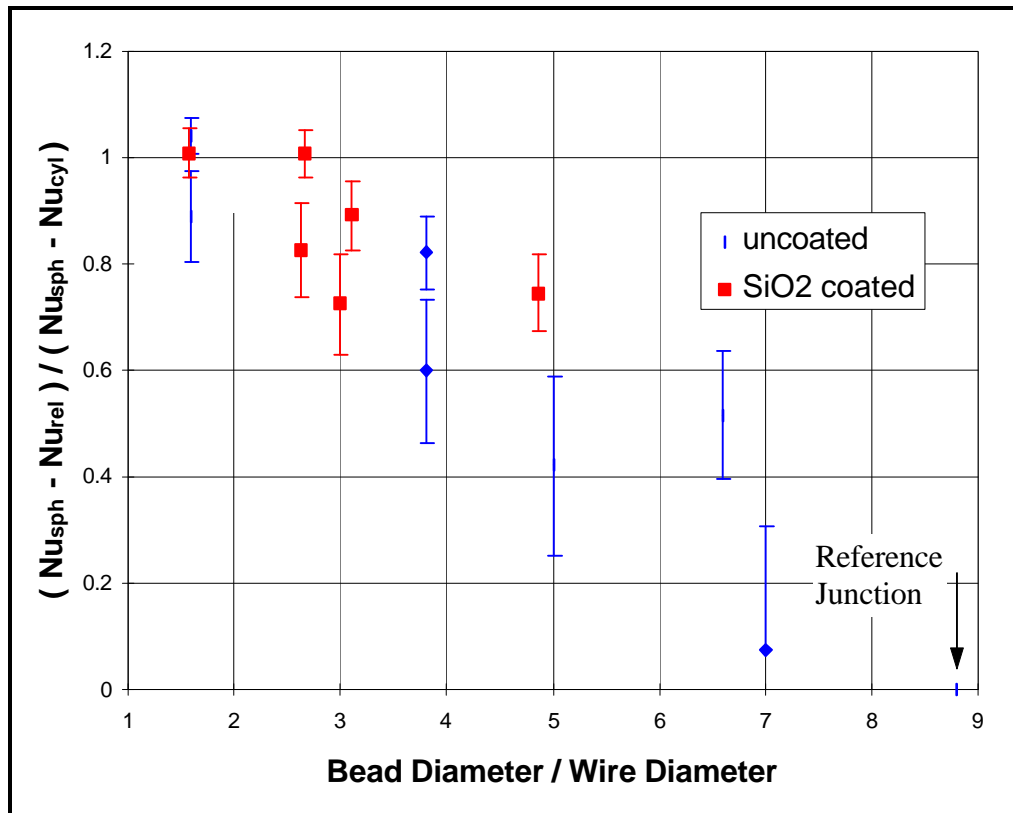


Figure A.10 Normalized Thermocouple Junction Nusselt Number Measurements vs. Nondimensionalized Junction Diameter, all 50 μ m Wire